Influence of Agglomeration of Nanoparticles on Tensile Strength and Wear Rate of AA6061/Graphite Metal Matrix Composites

A. Chennakesava Reddy

Professor, Department of Mechanical Engineering, JNT University, Hyderabad

Abstract: The inspiration for research in the development of metal matrix composites is their exceptional properties and performance over conventional metals and alloys. Some of the boosted properties of metal matrix composites include high specific strength and stiffness, better high temperature performance, low thermal expansion and high wear resistance. The tensile and wear behavior of an AA6061 matrix reinforced with graphite nanoparticles were investigated from an experimental and a theoretical point of view. An increase in ultimate tensile strength has been observed over the unreinforced metal. The strengthening mechanisms responsible for the improvement of mechanical properties of nano-reinforced metal matrix composites have been discussed. The graphite nanoparticles in the AA6061 matrix act as load-bearing fillers and group dislocations to harden the metal matrix. The reduced interparticle spacing is favorable to an increase in the work hardening rate due to obstruction to the dislocations by the agglomerations of graphite nanoparticles. In addition, pin-on-disc wear tests were conducted with different combinations of reinforcement, sliding distance, normal load, sliding speed as per the design experiments proposed by Taguchi. Based on the experimental results an empirical model was established. The graphite nanoparticles prevent the sticking or welding during sliding by way of forming a conductive tribo-layer between the composite pin and steel disc. The wear rate is decreased with increased volume fraction of graphite in AA6061 matrix. The results obtained from the empirical model are in good agreement with the experimental results.

Keywords: AA6061, graphite, applied load, sliding distance, sliding speed, wear, tensile strength.

1. Introduction

Metal matrix composites represent integrated combination of metallic and ceramic phases targeted to offer enhanced properties when compared to their unreinforced matrix metal. Aluminium composites are widely employed in the aerospace and automotive industries [1]. Ceramics such as silica [2], silicon carbide [3, 4], silicon nitride [5-8], titanium carbide [9-11], titanium boride [12-15], titanium oxide [16-18], titanium nitride [19], boron nitride [20], boron carbide [21, 22], magnesium oxide [23, 24], zirconium carbide [25], alumina trihydrate [26], graphite [27-31] and so on. The reinforcement may augment specific stiffness, specific strength, abrasion resistance, creep resistance, thermal conductivity, and dimensional stability. In the early nineteenth century, the graphite was used to reinforce natural rubber to increase the longevity of tires. Today, graphite is found in all aspects of domestic and industrial applications. It is used in inkjet printer ink, as reinforcements for natural and synthetic rubber, as an active agent in electrically conductive plastics, as a pigment in paints, coatings, cosmetics, etc. The graphite has high aspect ratio leading to higher surface area per unit volume. Thus, it provides more wettable surface area improving ease of dispersion. Cembrola [32] has studied the effects of mixing time and type of graphite on the resistivity of graphite – rubber composites. The strengthening mechanisms of titanium-graphite composites were investigated in another research work [9]. It was observed that some of graphite nanoparticles were dissolved into the titanium matrix as a solid solution element.

The issue of wear equations and modelling is debated on a regular but occasional basis. Many of these equations are based on young modulus or hardness in the wear process. An example of this type is due to Archard [33]:

$$W = Ks\,P/3H \quad (1)$$

where W is the worn volume, s is the sliding distance, P is the applied load, H is the hardness of the softer material and the ratio of the last two is often taken as the real contact area. K is stated to be a constant related to the probability that an encounter of two asperities produces a wear particle. Rhee [34] found that the total wear of a polymer-matrix is a function of the applied load F, speed V and sliding time t according to

$$\Delta W = KF^a \mathrm{V^b t^c} \quad (2)$$

where ΔW is the weight loss of the friction material and K, a, b and c are empirical constants. F is the applied load; v is the sliding speed; and t is the sliding time. In the present work, the total wear of a metal matrix composite is defined as a function of reinforcement volume fraction, applied load, sliding speed and sliding distance according to

$$W = K{v_f}^a F^b V^c S^d \quad (3)$$

where a, b, c and d are power law coefficients of reinforcement volume fraction (v_f), applied load (F), sliding speed (V) and sliding distance (S), respectively. K is the empirical constant.

In general, several factors affect the wear equations. The common factors varied for studying the wear behavior of metal matrix composites are applied load, sliding speed, sliding distance and reinforcement volume fraction [35-40]. The load greatly affects the rate of wear.

The noteworthy feature of the present work is that the graphite (Gr) was collected from waste black ink cartridges from inkjet printing. In order to develop an empirical wear models for AA6061/Gr composites and to study the influence of agglomeration of Gr nanoparticles, the wear tests were performed on pin-on-disc equipment. The design of experiments was based on Taguchi techniques [41, 42].

Table 1: Wear parameters and levels

Factor	Symbol	Level–1	Level–2	Level–3
Reinforcement, Vol.%	A	10	20	30
Load, N	B	10	20	30
Speed, m/s	C	2	3	4
Sliding distance, m	D	500	750	1000

2. Materials and Methods

The matrix material was AA6061. The reinforcement material was Gr nanoparticles of average size 100nm. AA6061/Gr composites were fabricated by the stir casting process and low pressure casting technique with argon gas at 3.0 bar. The composite samples were given H18 heat treatment. The heat-treated samples were machined to get cylindrical specimens of 10 mm diameter and 30 mm length for the wear tests. The levels chosen for the controllable process parameters are summarized in Table 1. The orthogonal array, L9 was preferred to carry out wear experiments (Table 2). Tensile tests were conducted on universal testing machine (UTM) to find ultimate tensile strength and fracture behaviour of the composites. A pin-on-disc type friction and wear monitor (ASTM G99) was employed to evaluate the friction and wear

behaviour of AA6061/Gr composites against hardened ground steel (En32) disc. Knoop microhardness was conducted before and after wear tests. Optical and scanning electron microscopy analyses were also carried out to find consequence of wear test AA6061/Gr composite specimens.

Table 2: Orthogonal array (L9) and control parameters

Treat	A	B	C	D
1	1	1	1	1
2	1	2	2	2
3	1	3	3	3
4	2	1	2	3
5	2	2	3	1
6	2	3	1	2
7	3	1	3	2
8	3	2	1	3
9	3	3	2	1

3. Results and Discussion

Two composite samples for each trial were tested on random basis according to design of experiments. The size distribution of Gr nanoparticles in the present work is shown in figure 1. The average nanoparticle size is 100 nm.

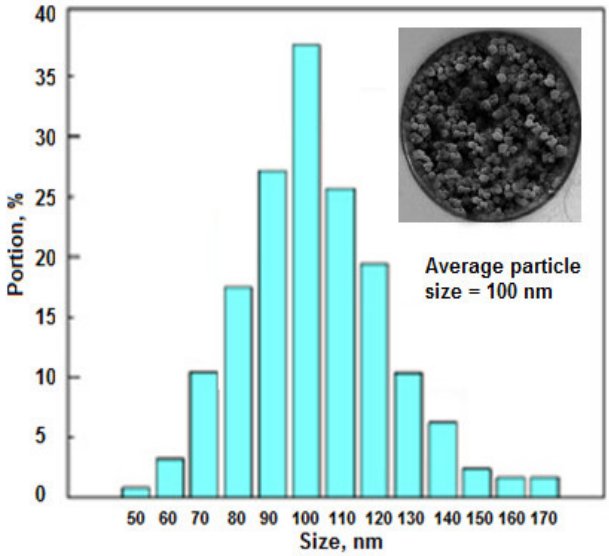

Figure 1. Size distribution of Gr nanoparticles

3.1. Tensile and Fracture Behaviour

The tensile strength increases with an increase of graphite content as shown in figure 2. For very strong particle-matrix interfacial bonding, Pukanszky et al. [43] presented an empirical relationship as given below:

$$\sigma_c = \left[\sigma_m \left(\frac{1-v_p}{1+2.5v_p}\right)\right] e^{Bv_p} \quad (4)$$

where B is an empirical constant, which depends on the surface area of particles, particle density and interfacial bonding energy. The value of B varies between from

3.49 to 3.87. This criterion has taken care of the presence of particulates in the composite and interfacial bonding between the particle/matrix. The effect of particle size and voids/porosity were not considered in this criterion. By considering adhesion, formation of precipitates, particle size, agglomeration, voids/porosity, obstacles to the dislocation, and the interfacial reaction of the particle/matrix, the formula for the strength of composite is stated by the author as below:

$$\sigma_c = \left[\sigma_m \left\{\frac{1-(v_p+v_v)^{2/3}}{1+2(v_{p+}v_v)}\right\}\right] e^{m_{p(v_p+v_v)}} + m_p d_p^{-1/2} \quad (5)$$

where υ_v and υ_p are the volume fractions of voids/porosity and nanoparticles in the composite respectively, m_p is the possion's ratio of the nanoparticles, d_p is the mean nanoparticle size (diameter) and σ_m is tensile strength of the matrix. The tensile strengths obtained by this model (with voids) and experimental results were almost equal. To get the composite strength, the load-bearing capabilities of both the metal and the reinforcement. The load transfer from the AA6061 matrix to the Gr nanoparticles under an applied external load contributes to the strengthening of the AA6061/Gr composites. For the equiaxed spherical particles, the load transfer is given by

$$\sigma_{lt} = V_f \sigma_m / 2 \quad (6)$$

From the above equation (6), the load transfer increases with increase in volume fraction of Gr. The grain size has a strong influence on the strength of composites since the grain boundaries can hinder the dislocation movement. The Hall-Petch equation relates the strength with the average grain size (d):

$$\sigma_{HP} = K/\sqrt{d} \quad (7)$$

where K is the strengthening coefficient. The increase of volume fraction and the decrease of d_p (particle diameter) lead to a finer structure. Because of Orowan mechanism, the non-shearable ceramic reinforcement particles pin the crossing dislocations and promote dislocations bowing around the particles under external load.

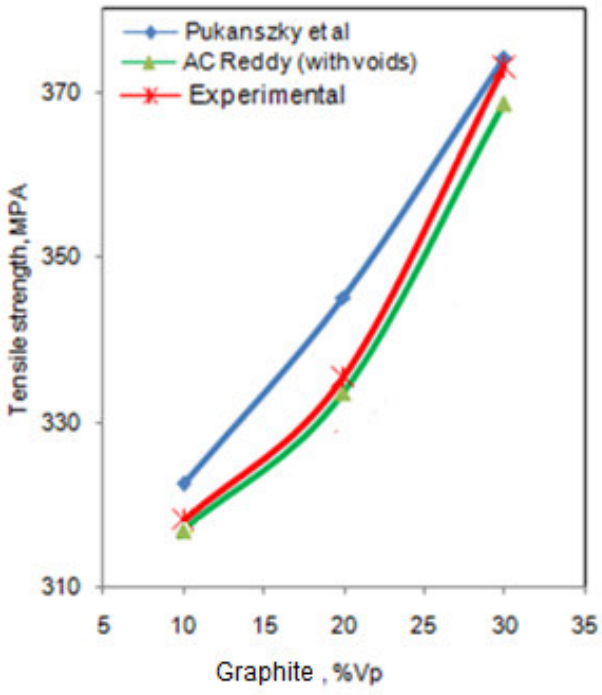

Figure 2. Effect of volume fraction on tensile strength

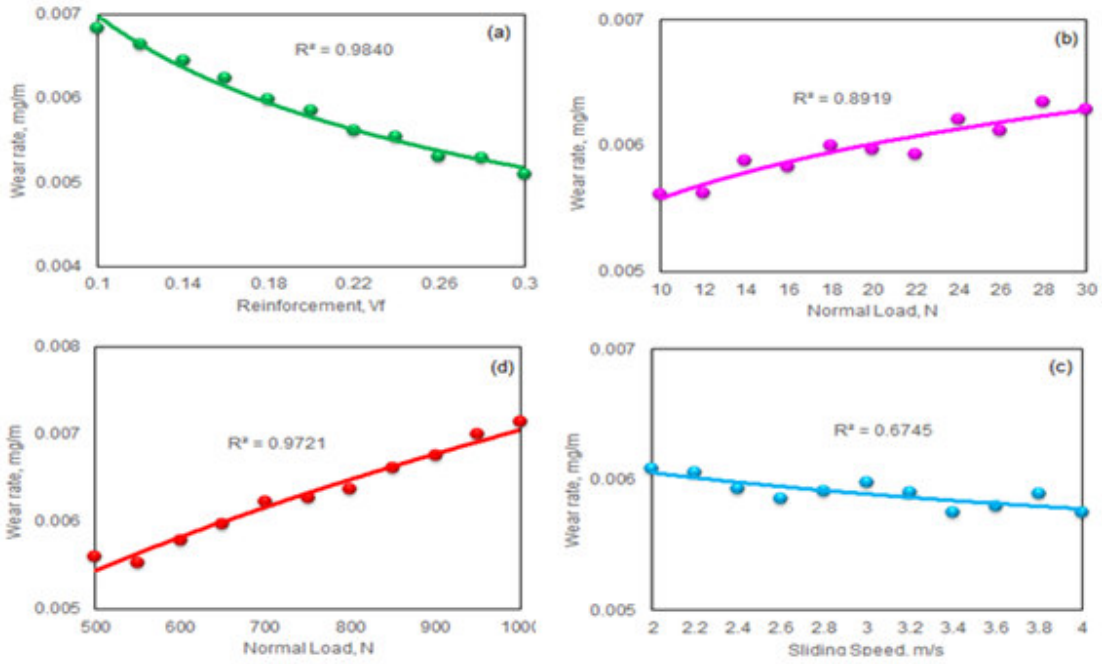

Figure 3: Influence of process variables on wear rate.

3.2. Wear Behaviour

The influence of vol.% Gr, applied load, sliding speed ad sliding distance are directly proportional to the slope of their graphs presented in figure 3. As observed from figure 3a, the wear rate is decreased with increased volume fraction of Gr in AA6061 matrix. This is on owing to the reduction of plastic deformation on the wearing surface. As seen from figure 3b, an increase in wear rate is with increase of load applied on the composite specimen due to extensive plastic flow of the AA6061matriax and substantial wear debris formation. The wear rate decreases with increase in sliding velocity for composites as shown in figure 3c. At low sliding speeds, the phenomena responsible to the wear rate is delamination theory. The reduction of wear rate at high speeds is self-lubrication behaviour of Gr nanoparticles. The Gr nanoparticles prevent the sticking or welding during sliding by way of forming a conductive tribo-layer between the composite pin and steel disc. It is also observed from figure 3d that the wear rate is proportional to the sliding distance. The higher wear rate was due to the adhesive wear of AA6061/Gr composite material on the sliding disc.

3.2 Significance of Process Variables on Wear Rate

For the AA6061/Gr composites, the weight loss function is determined using the wear rate as a reference value. The weight loss function is as follows:

$$W_L = k(W_y - W_m)^2 \quad (8)$$

In this equation, W_L is the loss associated with a particular wear rate value W_y, Wm is the nominal value of the wear rates, and the value of k is a constant depending on the wear rate at the specification limits and the width of the specification. For the variables mentioned in the present work, the weight loss functions are constructed as shown in figure 4. If the AA6061/Gr composite reaches the end of the upper safety limit (USL) or lower safety limit (LSL), the composite should be scrapped.

In order to distinguish the significance of variables, the wear tests were conducted as per the Taguchi's deign of experiments. The analysis of variance (ANOVA) is presented

in Table 3. The percent contribution indicates 49.13%, 10.35%, 1.50% and 39.00% of variation in the wear rate by the reinforcement volume fraction of Gr, applied load, sliding speed and sliding distance, respectively. The percent contribution of a particular variable indicates whether the performance of that variable is sensitive to bring variation in the wear rate. The major contribution is from the sliding distance seconded by vol.% Gr. Even though the sliding speed satisfies the fisher's test, its influences is negligible. However, the applied load has significant influence on the variation of wear rate of AA6061/Gr metal matrix composites.

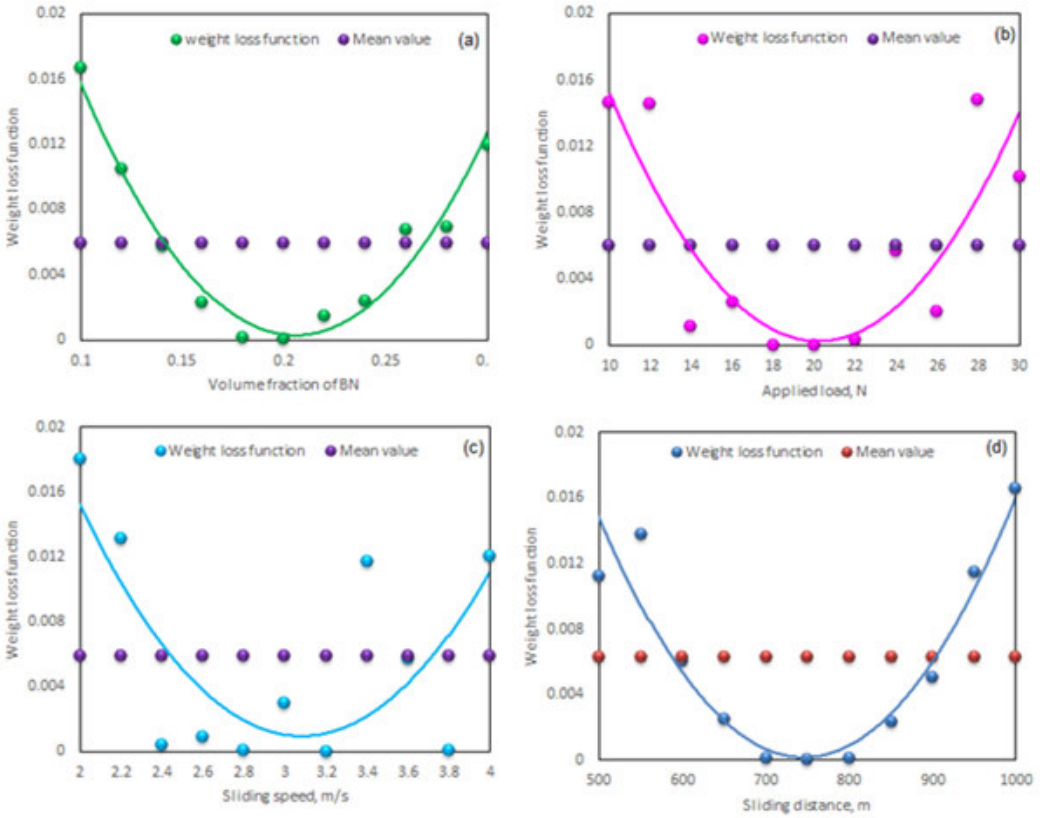

Figure 4: Weight loss functions of AA6061/Gr composites

Table 3: ANOVA summary of the effective stress

Source	Sum 1	Sum 2	Sum 3	SS	v	V	F	P
A	4.15E-2	3.46E-2	3.09E-2	9.53E-6	2	4.76E-6	7330.68	49.13
B	3.42E-2	3.43E-2	3.85E-2	2.01E06	2	1.00E-6	1544.21	10.35
C	3.67E-2	3.53E-2	3.50E-2	2.91E-7	2	1.45E-7	223.60	1.50
D	3.03E-2	3.72E-2	3.95E-2	7.56E-6	2	3.78E-6	5818.98	39.00
e				5.85E-9	9	6.50E-10		0.00
T	1.43E-1	1.41E-1	1.44E-1	1.94E-5	17			100.00

Note: SS is the sum of square, v is the degrees of freedom, V is the variance, F is the Fisher's ratio, P is the percentage of contribution and T is the sum squares due to total variation.

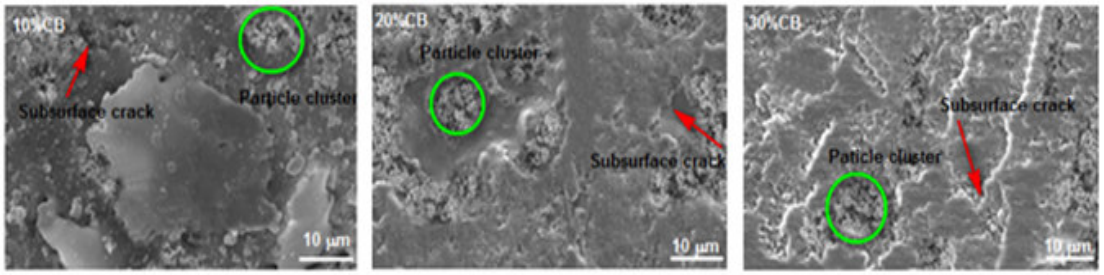

Figure 5: The worn surfaces of AA6061/Gr composites.

Figure 5 shows the worn surfaces of the AA061/Gr composites. The abrasive and adhesive wear mechanisms are predictable based on the worn surfaces. An increase in the reinforcement reduced the wear rate. The worn surfaces of AA6061/Gr composites reveal subsurface fracture, cavities and bounded Gr nanoparticles in the cavities. Some of the Gr particles have been pulled out from the cavities. The particle pull-out is due to the poor particle/matrix bonding. This was on account of the abrasive-wear mechanism of the composite material while resisting the delamination process. The wear resistance was greater in the case of composites having high volume fraction of Gr. The Knoop hardness was conducted on AA6061/Gr composite specimens (figure 6) before and after wear tests. The hardness values increase after wear test. The increase in hardness may be attributed to the reinforcement effect of Gr and work hardening during wear test on the pin-on-disc machine.

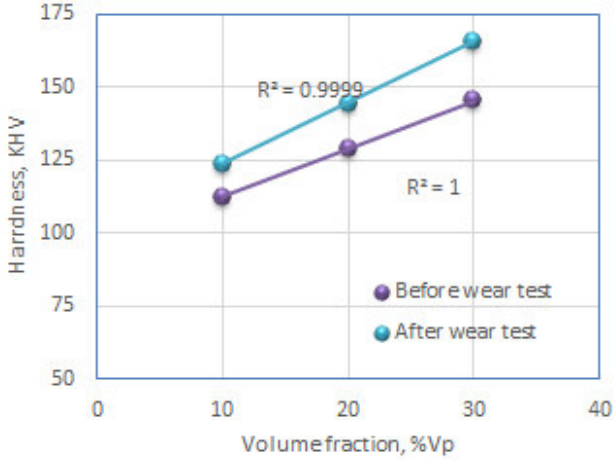

Figure 6: Hardness of AA6061/Gr composites after wear test.

The probability plots were created for each treatment by fitting with normal distributions and estimated the 87th percentile for each population as shown in figure 8. The estimated 87th percentiles for each population are:

- 0.006802 for the volume fraction of Gr,
- 0.006258 for the applied load
- 0.006027 for the sliding speed, and
- 0.006907 for sliding distance.

The estimated 87th percentiles indicate the merit of the factors A, B, C and D on the wear rate. The major contributing variables for the wear rate are the volume fraction of Gr and sliding distance. This confirms the ANOVA results of Taguchi's techniques except the order of sliding distance and volume fraction of Gr.

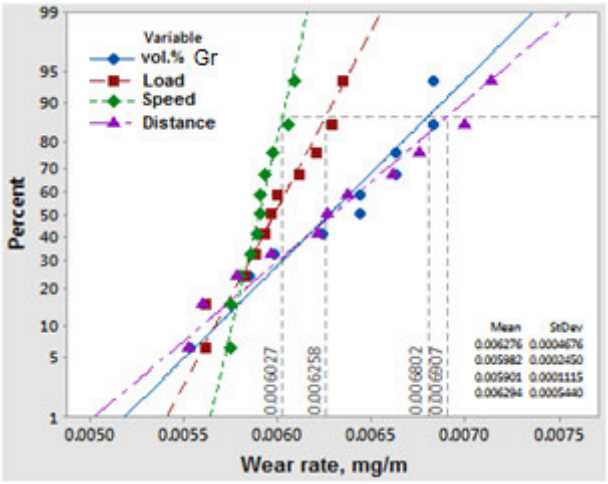

Figure 8. Probability analysis

3.3 Mathematical Modelling of Wear Rate

The mathematical relation between wear and volume fraction of reinforcement, applied load, sliding speed and sliding distance are obtained by curve fitting in terms of power laws as follows:

$$W_{rp} = 0.0037 v_f^{-0.2735} \quad (9)$$

$$W_{rf} = 0.0043 F^{0.1082} \quad (10)$$

$$W_{rn} = 0.0634 V^{-0.0679} \quad (11)$$

$$W_{rd} = 0.0005 S^{0.3738} \quad (12)$$

where, W_{rp} is the wear rate due to vol.% of reinforcement (v_f), mg/m; W_{rf} is the wear rate due to normal load (F), mg/m; W_{rn} is the wear rate due to speed (V), mg/m; and W_{rd} is the wear rate sliding distance (S), mg/m. The values of power law coefficients a, b, c and d are, respectively, -0.2735, 0.1082, -0.0679 and 0.3738 from Equations (9) to (12). By substituting the representative values of Vf, F, N and S and their corresponding power law coefficients on the right side of Equation (3) and substituting the experimentally obtained wear rates on the left side of Equation (3), the value of K is determined. The over-all wear rate (mg/m) equation for AA6061/Gr composites is given by

$$W = 7.8845 \times 10^{-4} \left(v_f^{-0.2735} F^{0.1082} V^{-0.0679} S^{0.3738} \right) \quad (13)$$

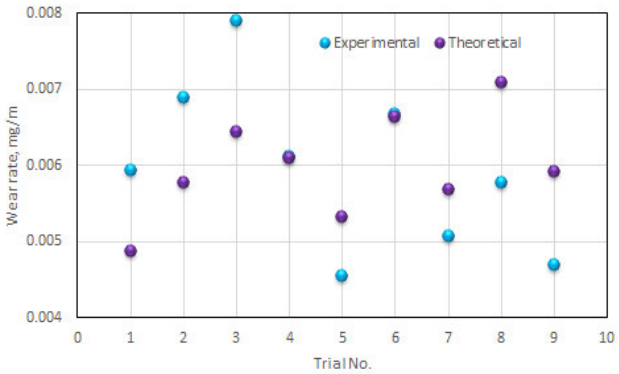

Figure 8: Comparison of experiments results with theoretical results.

The results obtained from the mathematical model are in good agreement with the experimental results as shown in figure 8. For the composites comprising of 10% Gr,

the results determined from the mathematical model are lower than the experimental results as the porosity is not considered in the mathematical modeling. The theoretical results are matching with those obtained experimentally for the case of 20% Gr nanoparticles in the composites. The results determined from the mathematical model are higher than the experimental results as the agglomeration is not considered in the mathematical modeling. The mathematical model assumes uniform distribution Gr nanoparticles in the AA6061 matrix without porosity.

4. Conclusions

The investigation on the tensile and wear behavior of AA6061/Gr nanoparticles reinforced metal matrix composites was carried out experimentally and theoretically. An increase in volume fraction of Gr nanoparticles has increased the hardness of the AA6061/Gr composites and subsequently enhanced the wear resistance. The tensile strength increases with an increase of graphite content. Due to agglomeration of Gr nanoparticles, the condensed interparticle spacing is favorable to an increase in the work hardening of AA6061/Gr composites. The worn surfaces of AA6061/Gr composites reveal subsurface fracture, cavities and bounded Gr nanoparticles in the cavities. The volume fraction of Gr and sliding distance are highly influential variables on the wear rate of composites. The wear rate decreases with the increase of volume fraction of Gr nanoparticles and decreases with the increase of sliding distance. The results derived from the predicted empirical model could match with those results acquired from the wear tests.

REFERENCES

[1] B.P. Krishnan, N. Raman, K. Narayanaswamy, and P.K. Rohatgi, Performance of An Al-Si Graphite Particle Composite Piston in a Diesel Engine, Wear, 60, pp. 205–215, 1980.

[2] A. C. Reddy, Thermal Expansion Behavior of Aluminum Matrix Composites Reinforced with Fused Quartz Nanoparticles, National Conference on Advanced Materials and Manufacturing Techniques, Hyderabad, 08-09th March 2004, 350-355.

[3] A. C. Reddy, Experimental Evaluation of Elastic Lattice Strains in the Discontinuously SiC Reinforced Al-alloy Composites, National Conference on Emerging Trends in Mechanical Engineering, Nagapur, 05-06th February 2004, pp.81.

[4] A. C. Reddy and B. Kotiveerachari, Effect of Matrix Microstructure and Reinforcement Fracture on the Properties of Tempered SiC/Al-Alloy Composites, National conference on advances in materials and their processing, Bagalkot, 28-29 November, 2003, pp.78-81.

[5] A. C. Reddy, Evaluation of Debonding and Dislocation Occurrences in Rhombus Silicon Nitride Particulate/AA4015 Alloy Metal Matrix Composites, 1st National Conference on Modern Materials and Manufacturing , Pune, India, 19-20 December 1997, 278-282.

[6] A. C. Reddy, Assessment of Debonding and Particulate Fracture Occurrences in Circular Silicon Nitride Particulate/AA5050 Alloy Metal Matrix Composites , National Conference on Materials and Manufacturing Processes, Hyderabad, India, 27-28 February 1998, 104-109.

[7] A. C. Reddy, Thermal Expansion Studies on Aluminum Matrix Composites with Different Reinforcement Volume Fractions of Si_3N_4 Nanoparticles, 4th International Conference on Composite Materials and Characterization, Hyderabad, India, 7-8 March 2003, 221-225.

[8] B. Kotiveera Chari, A. C. Reddy, Bottom-Up Pouring and its Effect on Porosity and Clustering in Casting of AA1100/Silicon Nitride Particle-Reinforced Metal

Matrix Composites, 6th National Conference on Materials and Manufacturing Processes, Hyderabad, 8-9 August 2008, pp. 110-114.

[9] S. Pitchi Reddy, A. C. Reddy, Effect of Needle-like Brittle Intermetallic Phases on Fracture Behavior of Bottom-up Poured AA5050/Titanium Carbide Particle-Reinforced Metal Matrix Composites, 6th National Conference on Materials and Manufacturing Processes, Hyderabad, 8-9 August 2008, pp. 127-132.

[10] A. C. Reddy, Local Stress Differential for Particulate Fracture in AA2024/Titanium Carbide Nanoparticulate Metal Matrix Composites, National Conference on Materials and Manufacturing Processes, Hyderabad, India, 27-28 February 1998, 127-131.

[11] A. C. Reddy, Effect of TiC Nanoparticles on the Coefficient of Thermal Expansion Behavior of the Aluminum Metal Matrix Composites, 5th National Conference on Materials and Manufacturing Processes, Hyderabad, 9-10 June 2006, 164-168.

[12] A. C. Reddy, Reckoning of Micro-stresses and interfacial Tractions in Titanium Boride/AA2024 Alloy Metal Matrix Composites, 1st International Conference on Composite Materials and Characterization, Bangalore, 14-15 March 1997, 195-197.

[13] A. C. Reddy, Prediction of CTE of Al/TiB_2 Metal Matrix Composites, 3rd International Conference on Composite Materials and Characterization, Chennai, India, 11-12 May 2001, 270-275.

[14] A. C. Reddy, Interfacial Debonding Analysis in Terms of Interfacial Tractions for Titanium Boride/AA3003 Alloy Metal Matrix Composites, 1st National Conference on Modern Materials and Manufacturing , Pune, India, 19-20 December 1997, 124-127.

[15] A. C. Reddy, Investigation of the Clustering Behavior of Titanium Diboride Particles in TiB_2/AA2024 Alloy Metal Matrix Composites, 4th International Conference on Composite Materials and Characterization, Hyderabad, India, 7-8 March 2003, pp.216-220.

[16] A. C. Reddy, Cohesive Zone Finite Element Analysis to Envisage Interface Debonding in AA7020/Titanium Oxide Nanoparticulate Metal Matrix Composites, 2nd International Conference on Composite Materials and Characterization, Nagpur, India, 9-10 April 1999, 204-209.

[17] A. C. Reddy, Stir Casting Process on Porosity Development and Micromechanical Properties of AA5050/Titanium Oxide Metal Matrix Composites, 5th National Conference on Materials and Manufacturing Processes, Hyderabad, 9-10 June 2006, 144-148.

[18] A. C. Reddy, Effect of Clustering Induced Porosity on Micromechanical Properties of AA6061/Titanium Oxide Particulate Metal matrix Composites, 6th International Conference on Composite Materials and Characterization, Hyderabad, 8-9 June 2007, pp. 149-154.

[19] A. C. Reddy, Effect of Porosity Formation during Synthesis of Cast AA4015/Titanium Nitride Particle-Metal Matrix Composites, 5th National Conference on Materials and Manufacturing Processes, Hyderabad, 9-10 June 2006, 139-143.

[20] Essa Zitoun, A. C. Reddy, Microstructure-Property Relationship of AA3003/Boron Nitride Particle-Reinforced Metal Matrix Composites Cast by Bottom-Up Pouring, 6th National Conference on Materials and Manufacturing Processes, Hyderabad, 8-9 August 2008, pp. 115-119.

[21] A. C. Reddy, Role of Porosity and Clustering on Performance of AA1100/Boron Carbide Particle-Reinforced Metal Matrix Composites, 6th International Conference on Composite Materials and Characterization, Hyderabad, 8-9 June 2007, pp. 122-127.

[22] A. C. Reddy, Effect of Particle Loading on Microealstic Behavior and interfacial Tractions of Boron Carbide/AA4015 Alloy Metal Matrix Composites, 1st International Conference on Composite Materials and Characterization, Bangalore, 14-15 March 1997, 176-179.
[23] A. C. Reddy, Constitutive Behavior of AA5050/MgO Metal Matrix Composites with Interface Debonding: the Finite Element Method for Uniaxial Tension, 2nd National Conference on Materials and Manufacturing Processes, Hyderabad, India, 10-11 March 2000, pp. 121-127.
[24] A. C. Reddy, Simulation of MgO/AA6061 Particulate-Reinforced Composites Taking Account of CTE Mismatch Effects and Interphase Separation, 3rd National Conference on Materials and Manufacturing Processes, Hyderabad, India, 22-25 February 2002, 184-187.
[25] A. C. Reddy, Effect of CTE and Stiffness Mismatches on Interphase and Particle Fractures of Zirconium Carbide /AA5050 Alloy Particle-Reinforced Composites, 3rd International Conference on Composite Materials and Characterization, Chennai, India, 11-12 May 2001, pp. 257-262.
[26] A. C. Reddy, Studies on fracture behavior of brittle matrix and alumina trihydrate particulate composites, Indian Journal of Engineering & Materials Sciences, 9, 2003, pp.365-368.
[27] A. C. Reddy, Micromechanical Modelling of Interfacial Debonding in AA1100/Graphite Nanoparticulate Reinforced Metal Matrix Composites, 2nd International Conference on Composite Materials and Characterization, Nagpur, India, 9-10 April 1999, 249-253.
[28] A. C. Reddy, Micromechanical and fracture behaviors of Ellipsoidal Graphite Reinforced AA2024 Alloy Matrix Composites, 2nd National Conference on Materials and Manufacturing Processes, Hyderabad, India, 10-11 March 2000, 96-103.
[29] A. C. Reddy, Behavioral Characteristics of Graphite/AA6061 Alloy Particle-Reinforced Metal Matrix Composites, 3rd International Conference on Composite Materials and Characterization, Chennai, India, 11-12 May 2001, 263-269.
[30] A. C. Reddy, Two dimensional (2D) RVE-Based Modeling of Interphase Separation and Particle Fracture in Graphite/5050 Particle Reinforced Composites, 3rd National Conference on Materials and Manufacturing Processes, Hyderabad, India, 22-25 February 2002, 179-183.
[31] A. C. Reddy, Finite Element Analysis Study of Micromechanical Clustering Characteristics of Graphite/AA7020 Alloy Particle Reinforced Composites, 4th International Conference on Composite Materials and Characterization, Hyderabad, India, 7-8 March 2003, 206-210.
[32] R. J. Cembrola, Relationship of graphite dispersion to electrical resistivity and vulcanizate physical properties, Polymer Engineering and Science, 22(10), 601-609, 1982.
[33] J. F. Archard, Contact and rubbing of flat surfaces, Journal of Applied Physics, 24, 981-988, 1953.
[34] S. K. Rhee, Wear equation for polymers sliding against metal surfaces, Wear, 16, 431-445, 1970.
[35] A. C. Reddy, Tribological Behavior of AA8090/MgO Composites, 5th National Conference on Materials and Manufacturing Processes, Hyderabad, 9-10 June 2006, 169-173.
[36] A. C. Reddy, On the Wear of AA4015 – Fused Silica Metal Matrix Composites, 4th International Conference on Composite Materials and Characterization, Hyderabad, India, 7-8 March 2003, 226-230.

[37] A. C. Reddy, Wear Characteristics of AA5050/TiC Metal Matrix Composites, National Conference on Advanced Materials and Manufacturing Techniques, Hyderabad , 08-09th March 2004, 356-360.
[38] A. C. Reddy, Significance of Testing Parameters on the Wear Behavior of AA1100/B4C Metal Matrix Composites based on the Taguchi Method, 3rd International Conference on Composite Materials and Characterization, Chennai, India, 11-12 May 2001, 276-280.
[39] A. C. Reddy, Wear and Mechanical Behavior of Bottom-Up Poured AA4015/Graphite Particle-Reinforced Metal Matrix Composites, 6th National Conference on Materials and Manufacturing Processes, Hyderabad, 8-9 August 2008, pp. 120-126.
[40] A. C. Reddy, Wear and Mechanical Behavior of Bottom-Up Poured AA4015/Graphite Particle-Reinforced Metal Matrix Composites, 6th National Conference on Materials and Manufacturing Processes, Hyderabad, 8-9 August 2008, 120-126.
[41] W. Wieleba, The statistical correlation of the coefficient of friction and wear rate of PTFE composites, Wear, 252, 719–729, 2002.
[42] A. C. Reddy, V. M. Shamraj, Reduction of cracks in the cylinder liners choosing right process variables by Taguchi method, Foundry Magazine, 10, 47-50, 1998.
[43] B. Punkanszky, B. Turcsanyi, F. Tudos, Effect of interfacial interaction on the tensile yield stress of polymer composites, In: H. Ishida, editor, Interfaces in polymer, ceramic and metal matrix composites, Amsterdam, Elsevier, 467-477, 1988.